Available online at www.sciencedirect.com
SCIENCE DIRECT
Surface & Coatings Technology 200 (2006) 6331 – 6335
SURFACE & COATINGS TECHNOLOGY
www.elsevier.com/locate/surfcoat

Plasma surface treatment of polyethylene terephthalate films for bacterial repellence

E. Amanatides [a], D. Mataras [a,*], M. Katsikogianni [b], Y.F. Missirlis [b]

[a] *Plasma Technology Laboratory, Department of Chemical Engineering, University of Patras, P.O. Box 1407, Patras 26504, Greece*
[b] *Laboratory of Biomechanics and Biomedical Engineering, Department of Mechanical Engineering and Aeronautics, University of Patras, Greece*

Available online 15 December 2005

Abstract

An investigation of the effect of PET surface treatment in He/O_2 rf discharges on the bacterial (*Staphylococcus epidermidis*) adhesion was performed. The study was carried out in constant discharge power conditions that allowed the isolation of the effect of gas pressure and bias potential. The increase of pressure and substrate bias was found to enhance the production of active species and ions in the discharge as well as the PET etch rate. Additionally, the surface roughness of all the plasma treated films, relative to the untreated PET, was higher at these conditions. However, no simple relation was found between bacterial adhesion and surface roughness. Plasma treatment is shown to significantly reduce bacterial adhesion to these surfaces and this is most probably associated with changes on the surface chemical structure and the surface energy.

Keywords: Plasma treatment; PET; *Staphylococcus epidermidis*; Adhesion

1. Introduction

Polyethylene terephthalate (PET) is used in certain medical devices due to its excellent mechanical properties and relatively high biocompatibility [1]. However, infection remains a major impediment to its long-term use, leading to significant morbidity and mortality [2]. The coagulase-negative staphylococci, most notably *Staphylococcus epidermidis*, have been identified as a predominant cause of infection in the immunocompromised host in the presence of a medical device [3]. Bacterial adhesion to medical devices may be reduced by altering the physicochemical interactions between the bacteria and the substrate surface [4]. As a result, a significant number of studies on improving the antibacterial properties of materials have focused on surface modification. Diamond-like carbon (DLC) coatings [5], silver (Ag) coatings [6], surface thiocyanation [7] and surfaces modified by various gas plasmas, such as argon and oxygen [8,9], have been proposed. Among these, plasma surface treatment presents major advantages; it is a very fast and economical process performed at room temperature, suitable for treating complex shapes, while it only modifies the surface of the material, the bulk properties remaining unaffected [10,11].

In this direction, the present work investigates the effect of the total gas pressure and the substrate bias on the surface morphology, etch rate and bacterial adhesion onto PET films, treated with 20% O_2 in He rf discharges. Several plasma diagnostics were applied in combination with measurements of the surface topography to reveal the changes of the PET treatment mechanism induced by the systematic variation of these parameters.

2. Experimental

The plasma treatment apparatus is a fully characterized cell from the electrical point of view. It consists of a 160-mm-diameter stainless steel chamber having two parallel round stainless steel electrodes with a diameter of 55 mm, equipped with four 50-mm quartz windows as described in Mataras et al. [12]. The interelectrode distance was kept constant at 25 mm and the treatment time was set at 15 min for all the experiments presented here. PET films with a thickness of 100 μm were mounted on the grounded electrode surface after being ultrasonically cleaned for 1 min in methanol.

* Corresponding author. Tel.: +30 2610997857; fax: +30 2610993361.
E-mail address: dim@plasmatech.gr (D. Mataras).

0257-8972/$ - see front matter © 2005 Elsevier B.V. All rights reserved.
doi:10.1016/j.surfcoat.2005.11.002

PET treatments were performed using a gas mixture of 20% O_2 in He under constant power conditions and with variable total gas pressures (10.67–67.7 Pa). The radiofrequency (rf) power provided by a 13.56 MHz generator (ENI ACG-3) was fed to discharge through a wattmeter (Diamond, SX200) and a proper impedance matching network, while a dc bias was applied to the substrate holder. Voltage (Hameg, model AZ92) and current (FCC model F-35-1) probes were used to acquire entire waveforms to a digital storage oscilloscope (Lecroy, model 9361) in order to determine the exact power consumed in the discharge, according to the method described in Spiliopoulos et al. [13]. Spatially resolved optical emission spectroscopy (SROES) was applied by moving the chamber and recording the light emitted from a certain portion of the discharge space with a resolution of 0.5 mm, as described in Mataras et al. [12]. In addition, laser reflectance interferometry (LRI) was employed for recording in situ the material etching rate [14]. For this purpose, a green solid state, diode laser (Ealing, Intelight 12M10) emitting at 532 nm was directed upon the polymer film and the reflected beam was collected and then recorded using a suitable photodiode.

The surface topography of native and plasma-modified PET films was examined by contact mode atomic force microscopy using a multimode AFM (Nanoscope III, Digital Instruments). The surfaces were analyzed by measuring the average surface roughness (*Ra*). Morphology studies were also carried out on a JEOL JSM 6300 Scanning Electron Microscope (SEM). The bacterial strain used in this study was the reference type culture *S. epidermidis* ATCC 35984 that produces slime. Before each experiment, bacterial cell concentration was adjusted to about a 3×10^8 colony forming units (CFU)/ml Dulbecco's phosphate-buffered saline (Gibco BRL), supplemented with 0.1 mg/ml $MgCl_2$ and 0.1 mg/ml $CaCl_2$, at pH 7.4, as described in Fonseca et al. [15]. Substrates were obtained by slicing native and plasma-modified PET into 1×1 cm^2 sections. These substrates were placed in a 24 well tissue culture plates containing 1 ml of the bacterial suspension and initial adhesion was allowed to occur under gentle shaking for 150 min at 37 °C. Quantification of bacterial adhesion on the film was conducted by the Colony Forming Units counting (CFU) method [15] and by SEM [16], after a gentle rinse to remove non-adherent or loosely adherent bacteria.

The effect of the various PET treatments on *Ra* and bacterial adhesion were statistically analyzed using the SPSS 12.0 package for Windows. In all cases, $p<0.05$ was chosen to denote the significance level.

3. Results and discussion

Different sets of electrical measurements were initially carried out at each pressure and for 0 and −30 V substrate bias voltage for determining constant power conditions. Namely, a drop of the applied voltage is required for maintaining constant power dissipation in the discharge with increasing total gas pressure. This leads to an increase of the discharge current and of the ohmic part of the discharge impedance, for both 0 and −30 V substrate bias voltages [13,17].

Furthermore, the change of the substrate bias from 0 to −30 V affects both the applied voltage and the current required for the same power consumption. In fact, the application of negative substrate bias imposes a drop of both the applied voltage and the discharge current at each pressure. This is mainly due to the change of the discharge impedance and the enhancement of the ohmic character of the discharge. This enhancement can also be attributed to a further increase of the electron–molecule collision frequency, which is related to a much more intense treatment of the PET surface under the negative bias conditions [18].

Moreover, SROES was applied for following the changes in the electron density and the collision frequency by recording the emission intensity distribution in space of He metastables (He*, $^3S–^3P^o$ 388.9 nm) and excited O atoms (O*, $^4P^o–^4D$, 338.1 nm). The production of He* requires electrons with energies higher than 19.8 eV, while O* are produced either from dissociative excitation of O_2 molecules (14.7 eV) or from the excitation of ground state O atoms (14 eV) [19,20]. Fig. 1(a) presents the spatial distribution of He* for the unbiased substrate and for different gas pressures. For the total gas pressures of 10.67 Pa and 16.67 Pa, the emission intensity is maximized at a distance of 11 and 9 mm from the rf electrode, respectively, and remains rather high close to the substrate holder. Further increase of pressure is followed by a displacement of the maximum towards the rf electrode and by

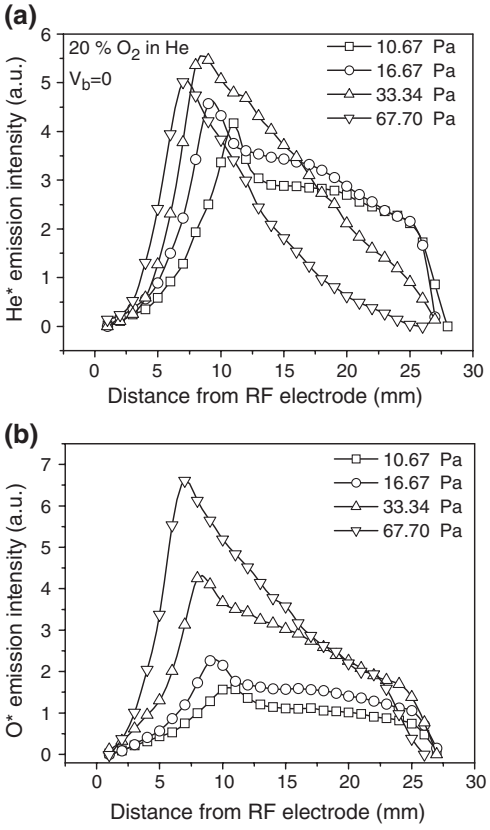

Fig. 1. Spatial profiles of (a) He metastables ($^3S–^3P^o$) and (b) O* atoms ($^4P^o–^4D$) for different O_2/He gas pressures and conditions of constant power dissipation and zero bias potential.

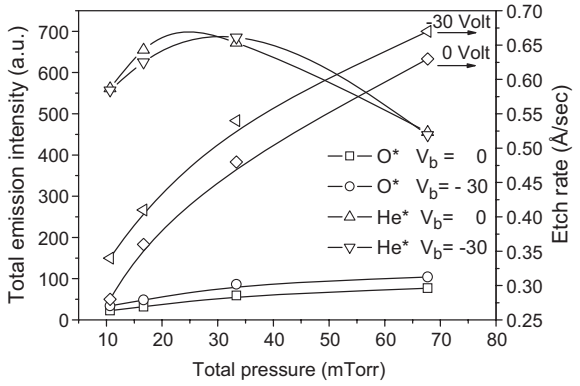

Fig. 2. Total He* and O* emission intensity (left axis) and PET etch rate (right axis) for 0 and −30 V substrate bias potential in constant power conditions.

a significant reduction of the emission intensity close to the substrate.

Fig. 1(b) presents the spatial distribution of O* under the same conditions. As in the case of He*, the increase of pressure shifts the maximum rate of production closer to the rf electrode. The position of the maximum is the same as in the He* distribution at each pressure; however, the increase of pressure does not seriously affect the emission intensity of O* close to the substrate. In fact, emission near the substrate is higher at 33.34 and 67.7 Pa and the intensity drop from the maximum to the substrate is not as sharp as in the case of He*. This difference can be explained by considering the different consumption pathways of He* and O* atoms in the He/O_2 discharges. He* have a significantly high lifetime, the main consumption path being the quenching of these species through collisions with the background gas or substrates. On the other hand, O_2 is an effective quencher of He* but the expected enhancement of quenching with pressure cannot explain the significant drop of He*, in particular close to the substrate. The drop, therefore, is mainly due to quenching of the excited species by the byproducts of PET treatment; a process that will be stronger close to the substrate and at higher pressures. On the other hand, the main O* consumption path is through spontaneous de-excitation, the lifetime of these species being of the order of a few nanoseconds.

Fig. 2 (left axis) presents the variation of the total He* and O* emission intensity, calculated by integrating the emission profiles of Fig. 1, as a function of gas pressure for both 0 and −30 V substrate bias. Concerning the O* species, the increase of pressure or the negative bias leads to an enhancement of the total emission intensity. The enhancement of the O* atoms density with pressure can be attributed to the increase of the electron density that was predicted from the electrical measurements and also to the increase of the O_2 density in the discharge. On the other hand, He* total emission intensity presents a broad optimum at pressures between 16.67 to 33.34 Pa, while in this case the negative substrate bias induces a slight drop of He* intensity. This is in agreement with the above discussion concerning the enhancement of the quenching rate at higher pressures due to the byproducts of the PET treatment.

An additional evidence of the stronger quenching of He* due to a more intense treatment of the PET surface at higher pressures comes also from the measurements of the PET etch rate presented in Fig. 2 (right axis). The etching rate increases with pressure, while it is further enhanced by the −30 V substrate bias. The effect of pressure on the etch rate can be due to the enhanced production of reactive oxygen species at higher pressures, as monitored with SROES for the O* atoms. An analogous enhancement can be expected for the production of ground state O atoms and O_2^+ ions taking into account the similar cross-sections of these processes. Both O atoms and O_2^+ ions can interact with the PET surface contributing to the observed increase of PET etch rate with either pressure or substrate bias.

Moreover, a change of the PET surface morphology is expected as a consequence of the observed etching. The surface topography of PET films was measured by AFM and Fig. 3 shows the micrographs of (a) the unmodified PET and (b) the unbiased PET films treated with 67.7 Pa, O_2/He discharges. The images were processed using the first-order flatten option. This

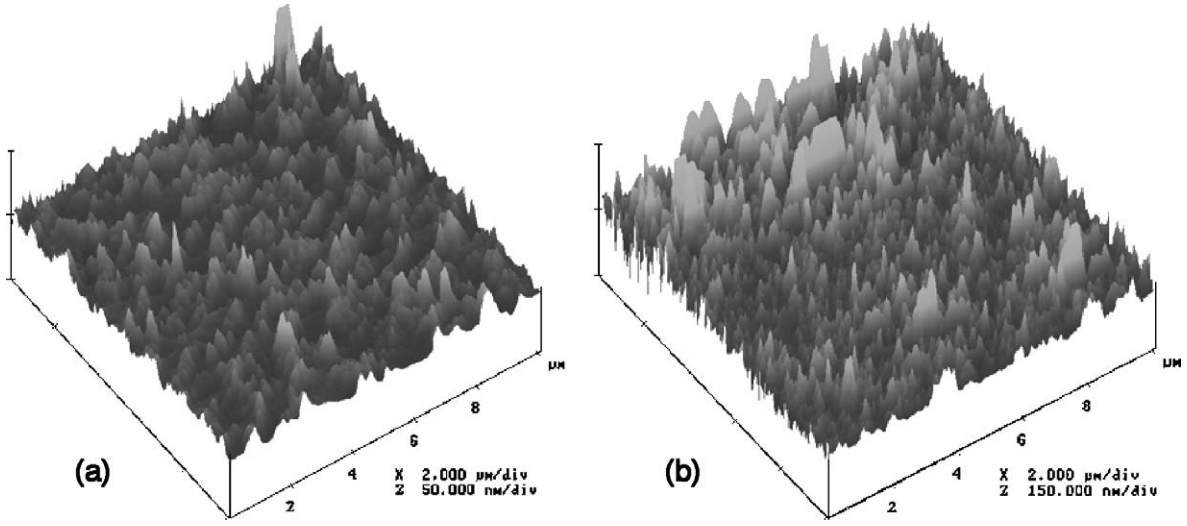

Fig. 3. AFM micrographs of: (a) untreated PET and (b) unbiased PET treated with 67.7 Pa, 20% O_2 in He discharges.

Table 1
Average surface roughness, *Ra*, and number of adhering bacteria for the unmodified PET film and the films treated under various gas pressures and substrate bias voltages

Sample	Roughness, *Ra* (nm)	Number of bacteria (cells/cm^2)
PET	2.72±1.13	9.58E6±0.99E6
P=10.67, V_b=0	9.72±4.03	–
P=16.67, V_b=0	11.62±3.76	3.80E6±0.96E6
P=33.34, V_b=0	7.33±1.46	2.30E6±0.62E6
P=67.70, V_b=0	18.95±3.93	3.20E6±0.73E6
P=10.67, V_b=30	6.16±3.51	3.90E6±0.16E6
P=16.67, V_b=30	5.88±0.56	2.90E6±0.37E6
P=33.34, V_b=30	11.26±2.73	3.80E6±0.43E6
P=67.70, V_b=30	13.29±0.82	3.50E6±0.46E6

The treated PET films code name is of the form: P=pressure, V_b=bias voltage.

option is available in the Nanoscope software (Digital Instruments) which was also used to generate *Ra* for a 10×10 μm^2 area images. The results show that unmodified PET surfaces are relatively smooth with granular structures of conical shape and moderate roughness. On the other hand, plasma-modified PET shows increased *Ra* mainly due to the enhancement of the already existing granular structures.

Furthermore, Table 1 summarizes the calculations of *Ra* for the PET films modified at different gas pressures and substrate bias conditions. It is remarkable that the *Ra* of all the treated films, although significantly higher than that of the unmodified PET, remains quite small (<20 nm), indicating the rather high stability of PET films against plasma treatment, as the phenyl ring is quite stable and contributes also to a global protection of the ester group from the attack of ions and reactive species [21]. In addition, the AFM results show that, for the films processed without bias, the increase of pressure up to 33.34 Pa slightly affects the surface roughness, while a further increase leads to an abrupt increase of *Ra*. In the case of −30 V, the situation is the same with the only difference that the sharp increase of *Ra* takes place for pressures higher than 16.67 Pa. In addition, the PET films treated under negative bias have lower surface roughness compared to the ones treated with no bias.

For the gas mixture used in this study, the most probable etching mechanism is ion-energy-driven [22]. Ions (O_2^+ and He^+) will have two roles in this mechanism: (a) to break surface bonds in order of their polarity through a recombination process and (b) to enhance the mobility of surface species, the adsorption of O atoms and consequently chemical etching or grafting. This mechanism can be highly anisotropic, enhancing thus the surface roughness in two limiting cases [22]:

(a) when the slow step of the process is the rate of arrival of O atoms at the surface, the ion flux is higher compared to the rate of byproducts desorption. However, this scheme does not explain the present results as the increase of pressure and the unbiased conditions leading to higher surface roughness, for sure does not favor the ion relative to O atoms flux,
(b) when the O atoms flux is higher compared to ion flux and both of them are higher compared to the rate of byproducts desorption. In this case, the horizontal etching rate will saturate when the surface coverage with byproducts becomes unity. On the other hand, the vertical etch rate will continue to increase and will be determined again by the ion flux to byproducts desorption ratio. This scenario describes better our results concerning the surface roughness as the increase of pressure favors the flux of O atoms and ions while the ion energy is lower for the case of unbiased compared to negatively biased conditions.

Finally, the number of adherent bacteria on the various surfaces was counted by SEM observation (Fig. 4) [16]. The same number approximately was found by the CFU method [15]. Table 1 summarizes the results of the bacterial adhesion to the different samples, showing that the highest number adhered on the unmodified PET, compared to all treated samples (p<0.05). It was observed, furthermore, that clusters of bacteria appeared on the unmodified PET (Fig. 4a) while on all treated samples the bacteria were isolated (Fig. 4b). No simple relation could be found between the surface roughness and the number of adherent bacteria probably due to the relatively small increase in *Ra* in all the modified samples. Owing to the high ionic strength of the buffer used for the bacterial suspension (0.256 M), the changes in the chemical structure that take place during plasma treatment of PET and concern the surface energy of the substrate [10,11,21,23] must be the important parameters that influence bacterial adhesion and accumulation. The increased substrate hydrophilicity of the treated PET, through the incorporation of oxygenated functional groups [9], seems to be the main reason for the reduced adherence of *S. epidermidis*,

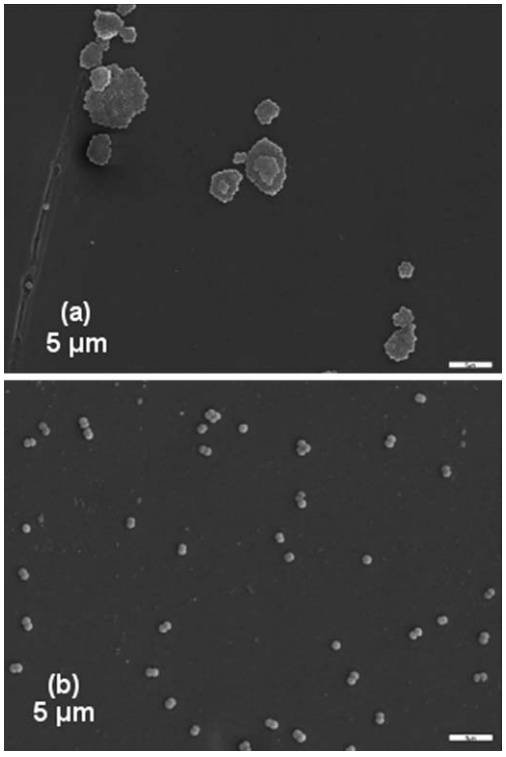

Fig. 4. SEM images of *S. epidermidis* cells deposited on (a) untreated PET ×2000 and (b) unbiased PET film treated with 67.7 Pa, 20% O_2 in He discharges ×2000.

a relatively hydrophilic bacterium [15], onto the modified PET [24]. Further work is in progress dealing with the effect of these parameters on the number of adhering bacteria and aiming at the determination of the main mechanism that governs the *S. epidermidis* adhesion and accumulation on the PET surface.

4. Conclusions

PET films were treated with He/O_2 discharges and under constant plasma power conditions in order to isolate as much as possible the effect of the total gas pressure and substrate bias potential on the PET etch rate, the surface morphology and the bacterial adhesion.

The production of excited O atoms was favored by the increase of pressure and the application of a negative bias voltage. An analogous increase of ground state O atoms and O_2^+ production was then estimated, which can explain the observed increase of PET etch rate with either pressure or substrate bias voltage.

Furthermore, plasma treatment of PET films was found to enhance surface roughness compared to the unmodified one. Higher pressure treatment and unbiased conditions favored the anisotropic etching and surface roughness. According to this observation, the most probable mechanism of PET etching under these conditions was proposed as the one where the O atoms flux is higher compared to the flux of ions while both of them are higher compared to the rate of byproducts desorption.

Finally, due to the relatively small changes, caused by the treatment, on the surface morphology and roughness, no simple relation was found between the surface morphology and bacterial adhesion. Actually, all the plasma-treated PET films significantly reduced bacterial adhesion. They probably prevent or delay biofilm formation as well, as evidenced by the isolated bacterial adherence. Therefore, the changes on the surface chemical structure and the surface energy due to plasma treatment seem to be the main reason for this behavior.

References

[1] M. Karck, L. Forgione, A. Haverich, Clin. Mater. 13 (1–4) (1993) 149.
[2] J.-L. Vincent, Lancet 361 (2003) 2068.
[3] C. Vuong, M. Otto, Microbes Infect. 4 (2002) 481.
[4] M. Hermansson, Colloids Surf., B Biointerfaces 14 (1999) 105.
[5] J. Wang, N. Huang, C.J. Pan, S.C.H. Kwok, P. Yang, Y.X. Leng, J.Y. Chen, H. Sun, G.J. Wan, Z.Y. Liu, P.K. Chu, Surf. Coat. Technol. 186 (2004) 299.
[6] D.P. Dowling, K. Donnelly, M.L. McConnell, R. Eloy, M.N. Arnaud, Thin Solid Films 398–399 (2001) 602.
[7] R. Nirmala, R. James, A. Jayakrishnan, Biomaterials 24 (2003) 2205.
[8] I.-W. Wang, M. Danilich, J. Anderson, R.E. Marchant, J. Biomed. Mater. Res. 29 (1995) 485.
[9] D.J. Balazs, K. Triandafillu, Y. Chevolot, B.-O. Aronsson, H. Harms, P. Descouts, H.J. Mathieu, Surf. Interface Anal. 35 (2003) 301.
[10] F. Arefi, V. Andre, P. Montazer-Rahmati, J. Amourouz, Pure Appl. Chem. 64 (1992) 715.
[11] R. d'Agostino, P. Favia, F. Fracassi, Plasma Processing of Polymers, Kluwer Academic Publishers, The Netherlands, 1997, p. 487.
[12] D. Mataras, S. Cavadias, D.E. Rapakoulias, J. Appl. Phys. 66 (1989) 119.
[13] N. Spiliopoulos, D. Mataras, D.E. Rapakoulias, J. Vac. Sci. Technol., A 14 (1996) 2757.
[14] E. Amanatides, S. Stamou, S. Boghosian, D. Mataras, Proceedings of the 16th European Photovoltaic Solar Energy Conference, Glasgow, UK, vol. I, 2000, p. 581.
[15] A.P. Fonseca, P.L. Granja, J.A. Nogueira, D.R. Oliveira, M.A. Barbosa, J. Mater. Sci., Mater. Med. 12 (2001) 543.
[16] Y.H. An, R.J. Friedman, J. Microbiol. Methods 30 (1997) 141.
[17] E. Amanatides, D. Mataras, J. Appl. Phys. 89 (2001) 1556.
[18] D.D. Papakonstantinou, E. Amanatides, D. Mataras, Proceedings of the 16th International Symposium on Plasma Chemistry (ISPC), Taormina, Italy, 2003.
[19] R.R. Laher, F.R. Gilmore, J. Phys. Chem. Ref. Data 19 (1990) 277.
[20] S. Rauf, M.J. Kushner, J. Appl. Phys. 82 (1997) 2805.
[21] P. Groning, M. Collaud, G. Dietler, L. Schlapbach, J. Appl. Phys. 76 (1994) 887.
[22] M.A. Lieberman, A.J. Lichtenberg, Principles of Plasma Discharges and Materials Processing, John Wiley & Sons, Inc., New York, 1994, p. 485.
[23] R. Cueff, G. Baud, J.P. Besse, M. Jacquet, J. Adhes. 42 (1993) 249.
[24] Y. Liu, S.-F. Yang, Y. Li, H. Xu, L. Qin, J.-H. Tay, J. Biotechnol. 110 (2004) 251.